TRENDS IN SCIENCES 2026; 23(6): 12279
https://doi.org/10.48048/tis.2026.12279 RESEARCH ARTICLE

Development and Comparison of Drying Tropical Herbal Strategies for *Annona muricata* Leaves: Integrating of Effective Moisture Diffusivity Using Antioxidant Activity, FTIR Ratios, and Color Attributes

Dessy Agustina Sari[1,2], Moh Djaeni[1,*], Devi Yuni Susanti[3], Joko Nugroho Wahyu Karyadi[4], Olly Sanny Hutabarat[5], Setia Budi Sasongko[1], Aji Prasetyaningrum[1] and Ching Lik Hii[6]

[1]*Department of Chemical Engineering, Universitas Diponegoro, Semarang 50275, Indonesia*
[2]*Chemical Engineering Program, Universitas Singaperbangsa Karawang, Karawang 41361, Indonesia*
[3]*Department of Food and Agriculture Products Technology, Universitas Gadjah Mada, Yogyakarta 55281, Indonesia*
[4]*Department of Agricultural Engineering and Biosystems, Universitas Gadjah Mada, Yogyakarta 55281, Indonesia*
[5]*Department of Agricultural Technology, Hasanuddin University, Makassar 90245, Indonesia*
[6]*Department of Chemical and Environmental Engineering, University of Nottingham, Selangor Darul Ehsan 43500, Malaysia*

([*]Corresponding author's e-mail: moh.djaeni@live.undip.ac.id)

Received: 14 October 2025, Revised: 27 October 2025, Accepted: 3 November 2025, Published: 30 January 2026

Abstract

Drying strategy employed exerts a significant influence on the kinetics and functional quality of *Annona muricata* (soursop) leaves. However, the current literature offers a paucity of practical, non-destructive indicators to inform process decisions. The present study sets out to compare sun drying (SD), room-temperature drying (RTD), convective tray drying (CTD; 40 - 60 °C), and microwave drying (MWD; 120 - 380 W), models thin-layer curves, and integrates effective moisture diffusivity (D_{eff}) with quality metrics - antioxidant activity (IC_{50}, DPPH), FTIR ratios (R_Q, R_1 - R_3), and color attributes (ΔE, a*). Multi-parameter models have been shown to outperform simpler forms. The Midilli model provided the most precise global fit ($R^2 > 0.95$; RMSE < 0.05), while Jenna-Das performed well in specific convective subsets. As the temperature/power were increased, D_{eff} increased and reached a peak at an MWD of 380 W. This resulted in an approximate acceleration of ~225× compared to the CTD 50 °C and a drying time of approximately ≈ 4 min. A clear trade-off emerged: CTD 40 °C exhibited a preserved appearance (ΔE ≈ 2.7) but under-retained phenolics (weaker IC_{50}), whereas CTD 60 °C and MWD 380 W produced higher ΔE (> 8) yet superior FTIR ratios (R_Q, R_1 - R_3) and stronger antioxidant activity; mid-power MWD (120 - 250 W) was detrimental. The colorimetric - spectroscopic linkages were found to be quantitative, with ΔE-IC_{50} exhibiting a weak-moderate relationship, and a* demonstrating a strong colleration with R_Q ($R^2 \approx 0.73$). Chemometrics (PLSR with VIP) identified R_Q/R_3 as dominant predictors ($R^2_{\{LOOCV\}} \approx 0.33$), thereby converting FTIR from descriptive readout to an actionable inline/at-line QC. Collectively, these results establish a predictive quality-control framework - using ΔE and a* with R_Q - for efficient selection, development, and implementation of tropical herbal drying technologies, and provide actionable set-points (optimal: MWD 380 W; convective alternative: CTD 60 °C) that balance speed and bioactive retention.

Keywords: Soursop leaves, Effective moisture diffusivity, IC_{50}, Thin-layer drying, FTIR ratio

Introduction

The utilization of tropical herbal leaves in functional foods and phytopharmaceuticals has increased in response to the demand for natural and sustainable products. While the drying process has been

demonstrated to extend shelf life, this stage can concomitantly result in a decline in phenolics and antioxidant capacity due to pigment conversion, oxidation, and structural degradation [1-6]. It has been demonstrated that microwave and freeze-drying techniques result in superior preservation of bioactivity when compared to conventional ovens. However, sun drying remains a viable option in tropical settings despite the high variability observed [7-12]. Consequently, there is a practical need for efficient drying strategies and non-destructive, predictive indicators that bridge laboratory analysis and industrial decision-making.

Annona muricata (soursop) leaves have been found to be rich in phenolics (e.g., gallic acid, catechin, quercetin, rutin) and flavonoids, supporting robust antioxidant activity and reported cytotoxic/anti-inflammatory effects that motivate their use in herbal teas and extracts [13-16]. However, post-harvest processing is fragmented: convective, solar, microwave, and other modalities have yielded variable outcomes for phenolics, antioxidant capacity, and color [17-19]. Consequently, a concise, integrative approach is imperative to balance process efficiency, speed, and bioactivity retention.

The quality of tropical herbal materials is commonly assessed via colorimetry (ΔE, a*) as markers of pigment/phenolic degradation, Fourier-transform infrared spectroscopy (FTIR) to track functional-group shifts associated with oxidation, and IC_{50} (DPPH) as a global indicator of radical-scavenging capacity [5,20-23]. Prior studies have frequently focused on a single indicator or a single drying method, thereby limiting comparative insight and rapid translation [24-27]. Emerging literature suggest that integrating color-FTIR-bioactivity may facilitate rapid, non-destructive prediction of herbal quality, particularly when combined with chemometrics [28,29,35,36]. However, such systematic integration has rarely been applied to *A. muricata* leaves. Three concise gaps emerge from this analysis: (i) limited cross-method evaluation of drying; (ii) insufficient integration of colorimetry and FTIR with bioactivity; and (iii) lack of rapid parameters suitable for real-time quality control.

In order to address these gaps, the present study introduces a multiscale integration of drying kinetics and modelling (sun/room drying; convective 40 - 60 °C; microwave 120 - 380 W) using established thin-layer models (Midilli, Page, Henderson-Pabis), with effective moisture diffusivity (D_{eff}) as a process-efficiency descriptor [30-34]. This study proposes a novel approach to predicting IC_{50} trends, offering a rapid and non-destructive surrogate for decision-making process. This study utilizes a combination of simple colorimetric indicators (ΔE, a*) with informative FTIR ratios (R_Q, R_1 - R_3) to achieve this objective, aligning with green processing principles and scalable quality control [28,29,35-39].

The objective of this research is 2-fold: (i) to evaluate the effects of temperature, power, and drying method on drying kinetics (thin-layer models, D_{eff}) and (ii) to assess product quality (IC_{50}, FTIR ratios, and color). Additionally, the study aims to quantify the structure–function relationships linking colorimetric parameters (ΔE, a*) and FTIR indices (R_Q, R_1 - R_3) with antioxidant capacity (IC_{50}). The results of this study are expected to (iii) enable a predictive quality control framework in which ΔE and a*, in combination with R_Q, serve as rapid and non-destructive indicators suitable for real-time process monitoring, and (iv) to provide actionable drying guidelines-comparing convective and microwave approaches - that balance process efficiency and phenolic retention for tropical herbal processing.

Materials and methods

Materials

Plant materials

Fresh soursop leaves *(Annona muricata*; **Figure 1**) were obtained from the cultivation garden of Diponegoro University, Tembalang, Semarang, Indonesia. The identification process was conducted in the Process Laboratory, and voucher specimens were stored for the purpose of taxonomic authentication. Prior to the commencement of the treatment, the leaf stalks were meticulously separated, the leaves were thoroughly washed and then stored at a temperature of 4 °C for 24 h. The samples were weighed (0.7 - 1.6 g on average) and their thickness was measured by means of a micrometer screw gauge (Mitutoyo, Japan; accuracy 0.1 mm). In each drying treatment, 30 g of fresh leaves were utilized (based on wet weight) with 3 replicates (n = 3).

Chemicals

Analytical-grade solvents (ethanol, methanol, n-hexane) were obtained from Merck (Germany). The standards of gallic acid, quercetin, and DPPH (2,2-diphenyl-1-picrylhydrazil) were obtained from Sigma-Aldrich (USA) and potassium bromide (KBr, ≥99%) was utilized for the preparation of FTIR pellets.

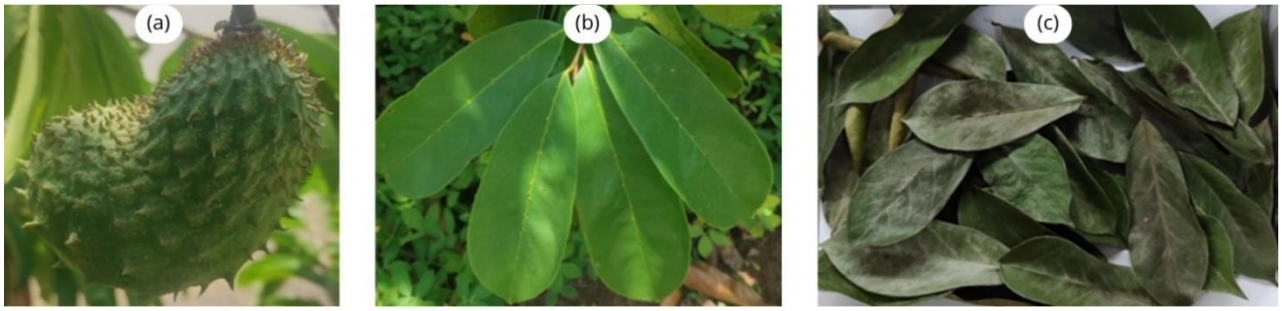

Figure 1 *Annona muricata*: (a) fruits, (b) fresh leaves, and (c) dry leaves.

Drying process

The drying treatments (**Figure 2**) comprised sun drying (SD), room temperature drying (RTD), convective tray drying (CTD), and microwave drying (MWD).

- Sun drying (SD). It was conducted in an outdoor environment between 9:00 a.m. and 3:00 p.m. A total of 30 g of the sample was placed into a thin cloth bag (30×23 cm^2) and placed on a stainless-steel tray (40×30 cm^2).
- Room temperature drying (RTD): It was conducted at room temperature between 27.5 and 31.1 °C with a relative humidity of 57.4% - 68.5%, in an indoor environment. The experiment was conducted from 08:00 a.m. to 16:00 p.m., and the temperature and humidity levels were monitored at regular intervals. The experiment was conducted in a way ascertaining protection from direct sunlight.
- Convective tray drying (CTD). It utilized a Sharp EO-35ST oven (Tokyo, Japan; 1000 W with maximum temperature at 250 °C). The oven was operated at temperatures of 40, 50, and 60 °C, with 75 mm between trays.
- Microwave drying (MWD). It was carried out using a Samsung MS20A3010AL microwave (Seoul, Korea; maximum 700 W) operated at 120, 250, and 380 W. A total of 30 g of the sample was spread evenly on a glass tray (205×205 mm^2).

Figure 2 Drying methods utilized: (a) SD, (b) RTD, (c) CTD, and (d) MWD.

During the drying process, the samples were weighed at regular intervals using electronic scales (D2B, PT Arta Joil Tappa, China; accuracy (0.01 g) until a constant weight was achieved (3 consecutive weighing with a variation of <0.1%). Time stamps were synchronized for subsequent MR-time analysis.

The modelling of the drying kinetics

The moisture ratio (MR)

The drying characteristics of the samples were evaluated using the moisture ratio (MR; Eq. (1)):

$$MR = \frac{X_t - X_e}{X_0 - X_e} \quad (1)$$

with X_t = moisture at time t, X_0 = initial moisture and X_e = equilibrium moisture [40].

Drying rate

The instantaneous rate was computed as Eq. (2):

$$\text{Drying rate} = \frac{X_{t+\Delta r} - X_t}{\Delta t} \quad (2)$$

Thin-layer drying models

This study involved the evaluation of seven models: Page, Henderson-Pabis, Logarithmic, Midilli, 2-term exponential, Diffusion approach, dan Jenna-Das [41-43]. The detailed equations are presented in **Table 1** with constants (a, b, c, k, k_0, k_1, n) estimated using non-linear regression.

Table 1 Thin-layer drying model.

Model	Equation
Page	$MR = \exp(-kt^n)$
Henderson and Pabis	$MR = a\exp(-kt)$
Logarithmic	$MR = a\exp(-kt) + b$
Midilli	$MR = a\exp(-kt^n) + bt$
2-term exponential	$MR = a\exp(-kt) + (1-a)\exp(-kat)$
Diffusion approach	$MR = a\exp(-kt) + (1-a)\exp(-kbt)$
Jenna-Das	$MR = a\exp(-kt) + b\sqrt{t} + c$

Effective moisture diffusivity (D_{eff})

The falling-rate period was modeled using Fick's Second Law for flat geometry (Eq. (3)):

$$MR = \frac{8}{\pi^2}\sum_{n=0}^{\infty}\frac{1}{(2n+1)^2}\exp\left[-\frac{(2n+1)^2\pi^2 D_{eff}t}{4L^2}\right] \quad (3)$$

where L refers to the average thickness of leaves and t denotes time. In practice, the first-term approximation was applied where appropriate to obtain stable D_{eff} estimates, while full-series fitting was checked for sensitivity.

Model adequacy and validation

The suitability of the model was evaluated by means of the coefficient of determination (R^2), root mean square error (RMSE), sum of squares error (SSE), and total sum of squares (TSS), with adequacy criteria of $R^2 > 0.95$ and RMSE < 0.05 [44,45].

$$MR = \frac{8}{\pi^2}\sum_{n=0}^{\infty}\frac{1}{(2n+1)^2}\exp\left[-\frac{(2n+1)^2\pi^2 D_{eff}t}{4L^2}\right] \quad (4)$$

$$SSE = \sum_{i=1}^{n}\left(MR_{exp,i} - MR_{pre,i}\right)^2 \quad (5)$$

$$TSS = \sum_{i=1}^{n}\left(MR_{exp,i} - \overline{MR_{exp,i}}\right)^2 \quad (6)$$

Residuals were screened for systematic deviation (runs/curvature). Models failing adequacy criteria were not advanced to comparative discussion.

Analysis of quality

Antioxidant activity (DPPH assay)

DPPH (2,2-diphenyl-1-picrylhydrazyl) is a stable radical used to assess radical-scavenging capacity. IC_{50} denotes the extract concentration (µg/mL) required to reduce DPPH absorbance by 50% - a smaller IC_{50} indicates stronger activity. With minor modifications to [46,47], leaf powder (1 g) was extracted in 20 mL 80% methanol using a digital sonicator (Elmasonic S30H, Germany) for 30 min, then filtered (Whatman No.1, 0.45 µm). An aliquot (2 mL extract) was mixed with 2 mL 0.1 mM DPPH, incubated 30 min in the dark, and absorbance was recorded at 517 nm (UV-Vis Shimadzu UV-1900, Japan). Inhibition (%) was computed by Eq. (7):

$$SSE = \sum_{i=1}^{n}\left(MR_{exp,i} - MR_{pre,i}\right)^2 \quad (7)$$

$$TSS = \sum_{i=1}^{n}\left(MR_{exp,i} - \overline{MR_{exp,i}}\right)^2 \quad (8)$$

where A_0 = control absorbance and A_1 = sample absorbance. The value of IC_{50} was determined from the

regression curves between the percentage of inhibition towards concentration.

FTIR spectroscopy

The spectrum was obtained using a PerkinElmer UATR Spectrum Two (US) in the range of 4,000 - 400 cm^{-1}, with a resolution of 4 cm^{-1}, scanned 32 times. The sample (in dry powder or fresh leaf pieces) was then placed directly on the ATR crystal. The main bands included O–H stretching, aliphatic C–H, ester/γ-lactone C=O, aromatic C=C, phenolic/ester C–O, and glycosidic C–O–C. Ratio indices R_1 - R_3 and the composite R_Q were computed from integrated band areas, modified from the Tepe method [48]. A consistent baseline and pathlength normalization were employed across runs.

Color analysis

The color coordinates (L, a*, and b*) were measured using a HunterLab ColorFlex EZ Colorimeter (USA) in accordance with CIE standards [49,50]. Derived indices such as ΔE, C, and h° were calculated for further analysis.

$$SSE = \sum_{i=1}^{n}\left(MR_{exp,i} - MR_{pre,i}\right)^2 \quad (9)$$

$$TSS = \sum_{i=1}^{n}\left(MR_{exp,i} - \overline{MR_{exp,i}}\right)^2 \quad (10)$$

$$\mathrm{C} = \sqrt{a^{*2} + b^{*2}}, h^{\circ} = \arctan\left(\frac{b^*}{a^*}\right) \quad (11)$$

Statistical analysis and software

All experiments were performed in triplicate (n = 3) with randomized drying order to minimize bias, and the results were presented as the mean ± standard deviation. Nonlinear regression on the drying curve was performed using Polymath 6.10 (USA), while IC_{50} values and color parameters were analyzed by means of one-way ANOVA followed by Tukey's test at a significance level of $p < 0.05$ (Minitab, Minitab LLC, USA). Treatment effects were also evaluated using Hedges' g effect size and linear and non-parametric relationships were tested with OLS regression and Spearman's correlation. To correlate rapid indicators with bioactivity, Partial Least Squares Regression (PLSR) (MATLAB R2024a, MathWorks, USA) was performed between FTIR indices (R_1 - R_3, R_Q) and IC_{50}. Leave-one-out cross-validation (LOOCV) was used to estimate predictive ability (reporting $R^2_{\{LOOCV\}}$ and RMSE), and Variable Importance in Projection (VIP) was computed to rank spectral predictors [51,52]. Chemometric adequacy was judged by stable VIP ranking (VIP $\gtrsim$ 1 considered influential) and the absence of pathological leverage.

Results and discussion

Drying process

Drying behavior and the factors of temperature/power

The MR-time curve (**Figure 3**) demonstrated that an augmentation in convective temperature (40 - 60 °C), microwave power (120 - 380 W), and sun-drying (SD) conditions significantly accelerated moisture release. RTD (29 °C) and CTD 40 °C were found at the slowest, requiring ≈ 30 - 33 h to reach MR = 0.10, while CTD 60 °C reached it in ≈ 4 h (≈ 64% faster than CTD 50 °C). SD appeared faster (~2.7 h) yet highly variable due to sunlight fluctuation. MWD 380 W has been observed as the most significant intensification, reducing drying time to ≈ 4 min (97% - 99% shorter than CTD 50 °C). The mean falling-rate slope (MR 0.60 - 0.20) substantiated this gradient: 0.025 $MR \cdot h^{-1}$ (CTD 40 °C) to 0.199 $MR \cdot h^{-1}$ (CTD 60 °C), 0.313 $MR \cdot h^{-1}$ (SD), and 0.036 - 0.226 $MR \cdot min^{-1}$ (MWD 120 - 380 W) (**Figure 4**; **Table 2** summarizes statistics).

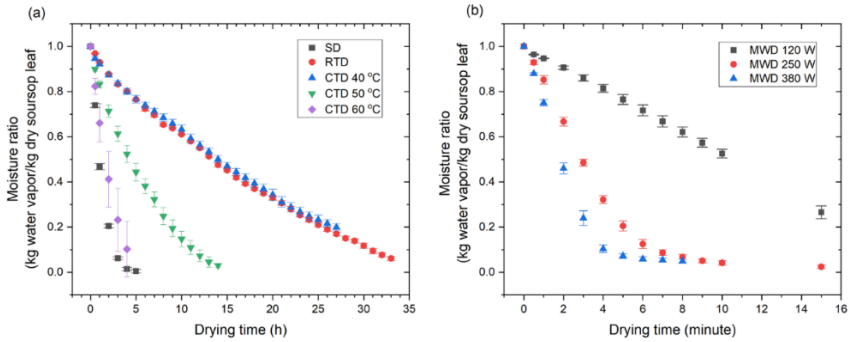

Figure 3 The moisture ratio during the drying process of soursop leaf.

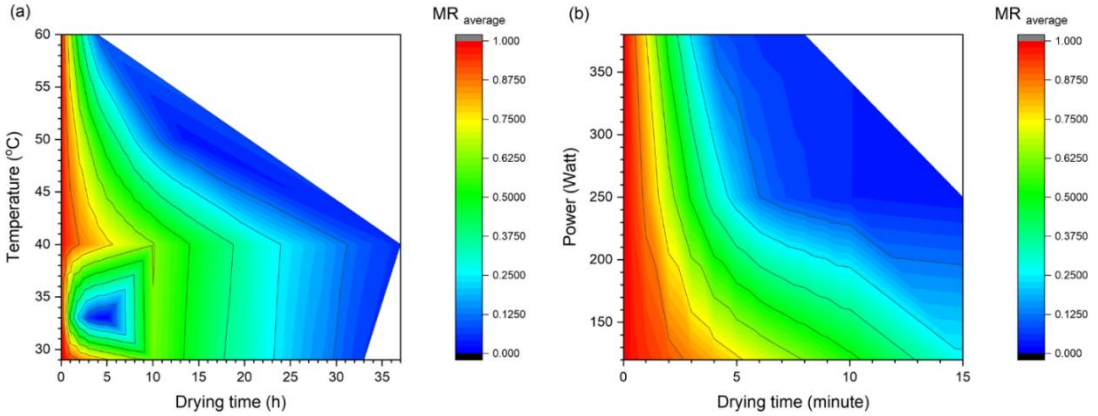

Figure 4 The plot of mean moisture ratio: (a) SD, RTD, CTD, and (b) MWD.

It is evident that all drying conditions follow a dominant falling-rate phase without a constant rate stage, which is typical of leafy matrices with robust internal diffusion resistance [42,53,54]. The enhancement observed at elevated CTD temperatures is consistent with findings reported for *Moringa oleifera* and holy basil [55,56]. The unreliability of SD is analogous to that observed in *Plantago lanceolata* and *Alcea rosea* [57,58]. In contrast, MWD generates volumetric heating (dipole rotation/ionic conduction), creating steep internal vapor-pressure gradients and microstructural disruption, as evidenced by celery and coriander [59,60]. It is noteworthy that an acceleration of up to ~225× (MWD 380 W vs. CTD 50 °C) is rarely reported for tropical medicinal leaves. However, it should be noted that each method has its limitations. The reliability of SD is compromised by the influence of UV/wind resulting in low reproducibility. MWD is susceptible to local overheating when the load is inadequate. RTD/CTD necessitate extended exposure and are vulnerable to phenolic degradation.

Thin-layer modelling

The multi-parameter nonlinear models (Midilli, Jenna-Das) demonstrated the highest level of accuracy ($R^2 \geq 0.994$; RMSE 0.006 - 0.026; **Table 2**; **Figure 5**). Jenna-Das demonstrated proficiency at RTD and at CTD 50 °C, while Midilli exhibited superiority at 40 °C; both exhibited comparable performance at 60 °C. Across MWD 120 - 380 W, Midilli was consistently superior ($R^2 > 0.995$). Drying constants increased with temperature/power (0.028 - 0.387 CTD; 0.020 - 0.311 MWD), while n decreased modestly (1.68 - 1.36).

Table 2 Constants-coefficients for fitted model and its statistical parameter for drying of soursop leaves.

Model	Statistical Parameter	SD, 33 °C	RTD, 29 °C	Temperature			Power MWD		
				CTD 40 °C	CTD 50 °C	CTD 60 °C	120 W	250 W	380 W
Page	k	0.7252	0.0303	0.0284	0.1419	0.3866	0.0200	0.1568	0.3106
	n	1.2223	1.2318	1.2475	1.1174	1.1974	1.5543	1.4108	1.3491
	R^2	0.9081	0.9878	0.9922	0.9935	0.9933	0.9893	0.9985	0.9935
	RMSE	0.1009	0.0322	0.0265	0.0250	0.0295	0.0429	0.0133	0.0260
Henderson and Pabis	k	0.8076	0.0614	0.0613	0.1785	0.4762	0.0815	0.2907	0.4523
	a	1.0322	1.0333	1.0370	1.0099	1.0324	1.0708	1.0697	1.0619
	R^2	0.9052	0.9767	0.9799	0.9904	0.9847	0.9703	0.9875	0.9868
	RMSE	0.1024	0.0445	0.0424	0.0305	0.0446	0.0714	0.0387	0.0371
Logarithmic	k	0.5580	0.0288	0.0353	0.1239	0.3570	0.0690	0.2792	0.4666
	a	1.1136	1.4875	1.2934	1.1620	1.1429	1.1569	1.0861	1.0539
	b	−0.1262	−0.5140	−0.3100	−0.1833	−0.1347	−0.0980	−0.0195	0.0115
	R^2	0.9840	0.9991	0.9989	0.9991	0.9962	0.9860	0.9877	0.9874
	RMSE	0.0421	8.54×10^{-3}	9.90×10^{-3}	9.51×10^{-3}	0.0221	0.0491	0.0385	0.0361
Midilli	k	0.7046	0.0511	0.0314	0.1577	0.3789	0.0135	0.1511	0.3103
	n	1.0385	0.8637	1.1290	0.9206	1.1018	1.6776	1.4358	1.3647
	a	1.0093	0.9940	0.9660	0.9928	0.9980	0.9612	0.9934	1.0017
	b	−0.0117	-8.83×10^{-3}	-2.96×10^{-3}	−0.0109	-9.92×10^{-3}	-6.89×10^{-4}	2.90×10^{-4}	7.62×10^{-4}
	R^2	0.9939	0.9995	0.9991	0.9993	0.9965	0.9979	0.9988	0.9952
	RMSE	0.0260	6.56×10^{-3}	9.15×10^{-3}	8.11×10^{-3}	0.0212	0.0188	0.0120	0.0224
Two-term exponential	k	1.0999	0.0584	0.0814	0.2232	0.6227	0.1256	0.4201	0.6491
	a	1.7808	1.0000	1.7631	1.6088	1.7233	1.9691	1.9411	1.9176
	R^2	0.9080	0.9747	0.9919	0.9943	0.9929	0.9861	0.9986	0.9943
	RMSE	0.1009	0.0464	0.0269	0.0235	0.0305	0.0488	0.0131	0.0243
Diffusion approach	k	0.7672	0.0237	0.0357	0.1205	0.3589	0.0595	0.2459	0.4515
	a	−2.9799	−2.9800	2.1046	−2.6285	−4.9600	−6.3755	0.9999	1.0000
	b	0.8263	0.8317	0.4777	1.2740	0.9466	0.8726	0.9998	0.9996
	R^2	0.9080	0.9887	0.9986	0.9982	0.9862	0.9872	0.9257	0.9818
	RMSE	0.1009	0.0311	0.0112	0.0133	0.0424	0.0468	0.0945	0.0435
Jenna-Das	k	0.7672	0.0237	0.0357	0.1205	0.3589	0.0595	0.2459	0.4515
	a	0.8696	1.3176	1.3543	0.9498	1.3192	1.4092	1.2501	1.0795
	b	−0.1000	−0.0301	6.92×10^{-3}	−0.0584	0.0536	0.0209	0.0293	6.30×10^{-3}
	c	0.1567	−0.3158	−0.3780	0.0477	−0.3206	−0.3795	−0.2015	−0.0181
	R^2	0.9940	0.9996	0.9989	0.9995	0.9966	0.9896	0.9899	0.9878
	RMSE	0.0257	5.83×10^{-3}	9.79×10^{-3}	6.81×10^{-3}	0.0211	0.0423	0.0348	0.0355

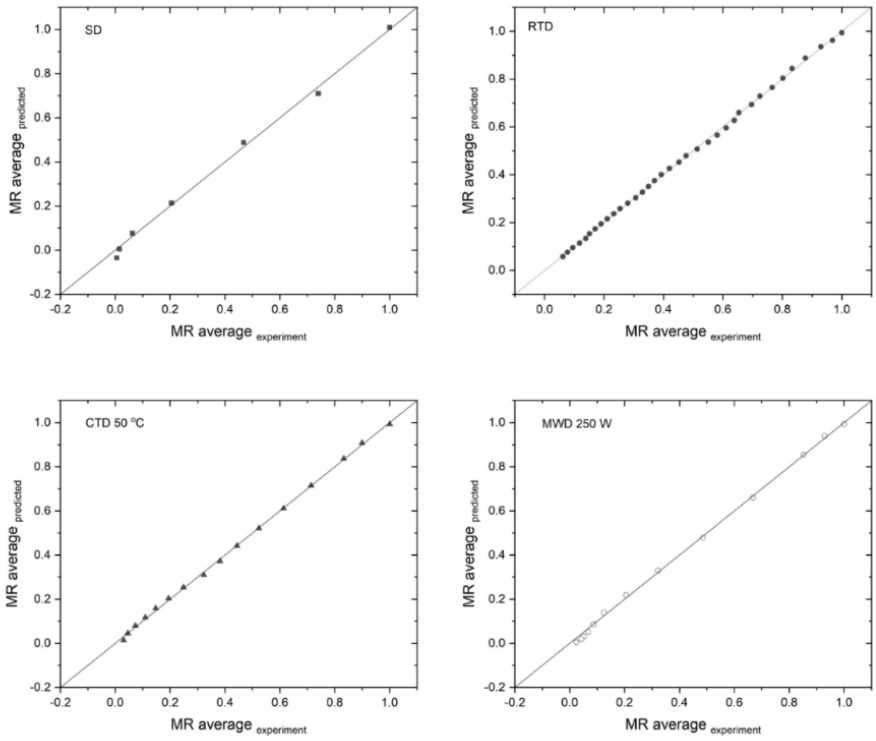

Figure 5 Comparison of MR experiment and Midilli modelling in the drying process of soursop leaf.

These findings emphasized the Midilli model as a universal predictive tool suitable for scale-up, while the Jenna-Das model remains more appropriate for convective subsets, consistent with the behavior observed in *Cosmos caudatus* and *Vernonia amygdalina* [61,62]. However, as empirical constructs, these models do not explicitly account for morphology or porosity evolution during drying process. Consequently, cross-batch validation is imperative, with particular consideration for variations in leaf thickness and ambient relative humidity, is required to ensure the adequacy of the input range and maintain predictive reliability.

Effective moisture diffusivity (D_{eff})

As demonstrated in **Table 3**, D_{eff} exhibited a marked increase with both temperature and microwave power: From 1.92×10^{-15} m^2/s (RTD) and 2.34×10^{-15} m^2/s (CTD 40 °C) to 1.26×10^{-13} m^2/s (CTD 60 °C); SD yielded 2.14×10^{-13} m^2/s; MWD 120 - 380 W reached 2.07×10^{-13} to 3.40×10^{-12} m^2/s (≈ 8.1 - 225×CTD 50 °C). The increase is indicative of lower viscosity, higher vapor pressure, and micro-cracks formation under higher thermal/microwave energy.

Table 3 Effective moisture diffusivity of soursop leaf.

Sample	D_{eff}, m^2/s	R^2	Relative to CTD 50 °C (fold)
SD	2.142×10^{-13}	0.989	14.19
RTD	1.924×10^{-15}	0.951	0.13
CTD 40 °C	2.343×10^{-15}	0.958	0.16
CTD 50 °C	1.509×10^{-14}	0.959	1.00
CTD 60 °C	1.263×10^{-13}	0.983	8.37
MWD 120 W	2.067×10^{-13}	0.940	13.70
MWD 250 W	1.225×10^{-12}	0.947	81.15
MWD 380 W	3.400×10^{-12}	0.942	225.13

At 380 W, the effective moisture diffusivity (D_{eff}) exhibited a 2 to 3 orders of magnitude increase compared to the CTD, a finding consistent with observations reported for *C. nardus* and *C. roseus* [33,63]. Its strong correlation with the falling-rate slope and the time required to reach MR = 0.10 highlights D_{eff} as a practical descriptor of drying efficiency. As demonstrated in relevant literature, elevated D_{eff} values under MWD conditions have been shown to be associated with enhanced phenolic retention and superior color preservation [64,65]. However, the accuracy of D_{eff} estimation is contingent upon the accuracy of geometry and thickness assumptions, and the reliability of the estimation is potentially compromised by the presence of uncontrolled external factors in the SD conditions.

Antioxidant activity (the assay of DPPH, IC_{50})

IC_{50} exhibited significant variation among treatments (**Figure 6(a)**), confirming a strong drying-method effect (ANOVA, F = 1,557.83; $p < 0.001$; $\eta^2 = 0.999$; **Table 4**). Fresh leaves demonstrated the lowest antioxidant activity (≈ 546 µg/mL), whereas MWD 380 W exhibited the strongest potential (≈ 107 µg/mL; ~5-fold improvement). The CTD 60 °C (~183 µg/mL) demonstrated superior performance in comparison to CTD 40 - 50 °C (~210 - 236 µg/mL), while RTD exhibited the weakest performance (~292 µg/mL). Tukey analysis categorized treatments into distinct groups, and Hedges' g revealed substantial contrasts, particularly between MWD 380 W and other methods (**Table 5**). A salient observation is that medium microwave power (120 - 250 W) yielded unanticipated IC_{50} values (≈ 310 - 333 µg/mL), indicating that mid-level energy prolongs exposure and expedite oxidative degradation, resulting in a U-shaped response. Conversely, high microwave intensity (i.e. ≥ 380 W) generates sufficient volumetric heating to reduce residence time and preserve bioactivity (**Figure 6(a)**). The IC_{50}-ln(D_{eff}) relationship was weak and insignificant ($R^2 = 0.06$; $\rho = -0.14$; **Figure 6(b)**; **Table 6**), indicating that kinetic intensification alone is inadequate to predict antioxidant preservation.

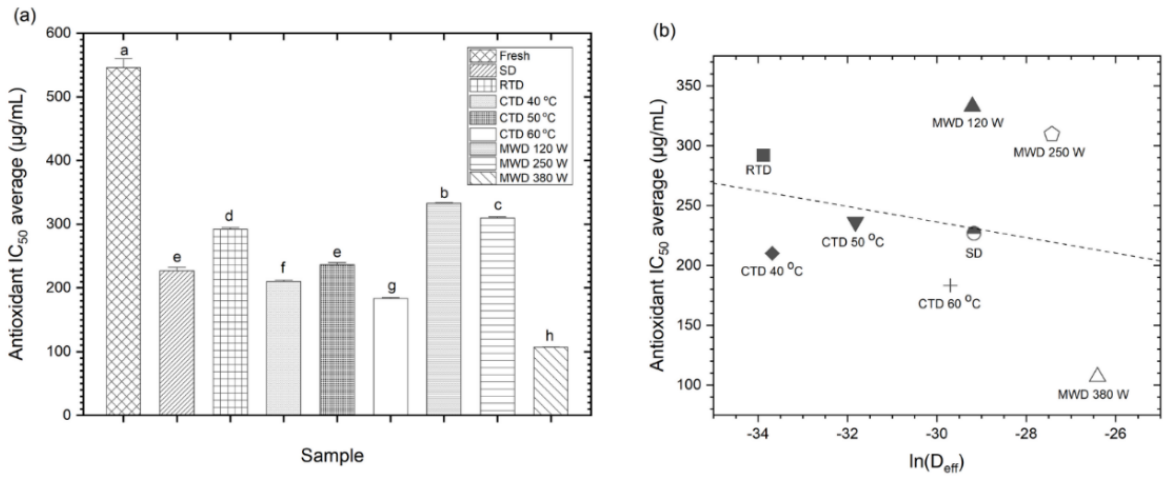

Figure 6 Soursop leaf: (a) anti-radical activity value, and (b) correlation of IC_{50}-ln(D_{eff}).

Table 4 ANOVA results regarding the effects of drying method on soursop leaf.

Source of variation	SS	df	MS	F	*p*-value	F-crit
Between Groups	368,170.4211	8	46,021.30263	1,557.8299	5.9164E-24	2.51015789
Within Groups	531.7549217	18	29.54194009			
Total	368,702.176	26				

Table 5 Level of Hedges' effects g (CI 95%) for the contrast of main IC_{50} among treatments.

Contrast	Hedges' g	95% CI	Interpretation
MWD 380 W vs Fresh	−35.09	[−59.45, −10.74]	Very large, significant
MWD 380 W vs SD	−23.28	[−39.46, −7.10]	Large, significant
MWD 380 W vs RTD	−85.42	[−114.63, −26.21]	Very large, significant
MWD 380 W vs CTD 40 °C	−55.51	[−94.00, −17.02]	Very large, significant
MWD 380 W vs CTD 50 °C	−41.78	[−70.76, −12.80]	Very large, significant
MWD 380 W vs CTD 60 °C	−48.58	[−82.27, −14.89]	Very large, significant
MWD 380 W vs MWD 120 W	−198.36	[−335.83, −60.90]	Extremely large, significant
MWD 380 W vs MWD 250 W	−97.35	[−164.82, −29.88]	Extremely large, significant
CTD 60 °C vs Fresh	−28.78	[−48.77, −8.80]	Very large, significant
CTD 60 °C vs SD	−8.12	[−13.89, −2.35]	Moderate, significant
CTD 60 °C vs RTD	−41.51	[−70.31, −12.72]	Very large, significant
CTD 60 °C vs CTD 40 °C	−11.29	[−19.21, −3.36]	Large, significant
CTD 60 °C vs CTD 50 °C	−15.47	[−26.27, −4.67]	Large, significant
SD vs Fresh	−23.60	[−40.00, −7.20]	Large, significant
SD vs CTD 50 °C	−1.60	[−3.29, 0.10]	Small, not significant

Table 6 Correlation of IC_{50} to $\ln(D_{eff})$ using OLS regression and Spearman correlation.

Analysis	Parameter	Value	Note
OLS regression	Intercept (β_0)	41.33	± 322.47 (SE)
	Slope (β_1)	−6.50	± 10.65 (SE)
	t(β_1)	−0.610	df = 6
	p-value	0.564	Not significant
	R^2	0.058	Weak
	R^2_{adj}	−0.099	Negative (small n or poor fit)
Spearman correlation	ρ	−0.142	Weak negative
	t	−0.353	df = 6
	p-value	0.736	Not significant

This nonlinear response has been documented in phenolic-rich matrices, where mid-level MWD induces oxidative stress, while higher microwave power enhances retention [66,67]. Similarly, moderate CTD temperatures (50 - 70 °C) often better preserve polyphenols compared to prolonged low-temperature drying or sun drying [5,68-70]. However, the DPPH assay only reflects overall antioxidant capacity and does not differentiate specific molecular contributors; thus, identifying individual compounds such as flavonoids or acetogenins requires further analysis using HPLC or LC-MS techniques.

FTIR analysis of phytochemical retention

FTIR spectra (**Figure 7**) displayed characteristic lignocellulosic-phenolic bands: O–H (3,280 - 3,300 cm^{-1}), aliphatic C–H (2,920/2,850 cm^{-1}), aromatic C=C (1,595 - 1,600 cm^{-1}), C–O (1,050 - 1,030 cm^{-1}), and glycosidic C–O–C (1,236 - 1,240 cm^{-1}). In comparison with fresh leaves (O–H at 3,289 cm^{-1}), dried samples exhibited a red shift (3,269 - 3,295 cm^{-1}) and diminished

O–H/C–O intensities, indicating weakened H-bonding and partial phenolic loss. A distinct C=O band (~1,734 cm^{-1}) emerged exclusively after drying (SD–MWD 380 W), thereby indicating oxidation/esterification. At 380 W, the weakening at 1,236 - 1,240 cm^{-1} signified partial polysaccharide depolymerization.

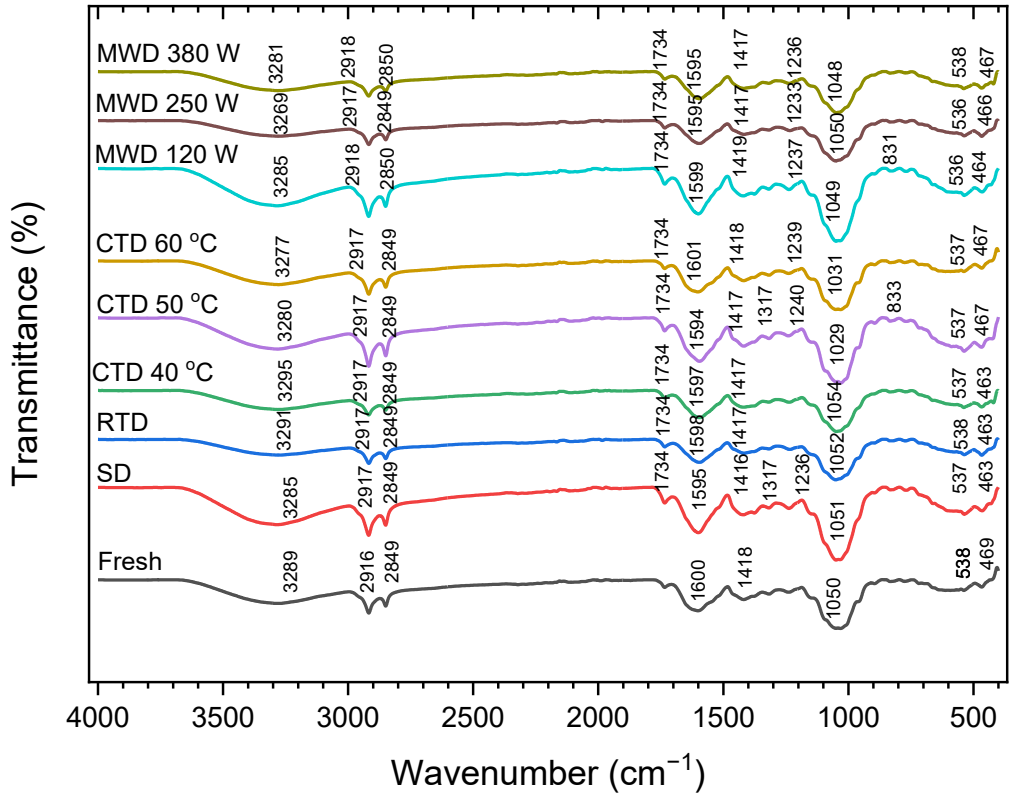

Figure 7 FTIR spectra of soursop leaf.

To capture these shifts quantitatively, ratios R_1–R_4 and a composite R_Q were proposed (**Figures 8(a)** and **8(b)**). R_Q demonstrated the strongest consistency with IC_{50} and outperformed single-band indicators, thereby transforming FTIR analysis from a purely descriptive tool into an in-line quality control (QC) approach. Analogous correlations between FTIR indices and antioxidant capacity have been reported for *Centella asiatica*, *Moringa oleifera*, black carrot, dates, and apples [48,71-76]. Integration with chemometric modeling further reinforced this framework: PLS regression analysis between FTIR predictors and IC_{50} yielded $R^2_{\{LOOCV\}}$ = 0.325 and RMSE = 95.9 µg/mL. VIP scores identified R_3 and R_Q as dominant predictors (**Figures 8(c)** - **8(d)**), thereby confirming that the phenolic-carbonyl equilibrium plays a pivotal role in antioxidant retention [77-82]. However, FTIR provides only spectral proxies; LC-MS or HPLC remains necessary to identify specific phenolic subclasses, and PLSR is sensitive to preprocessing steps such as baseline correction and normalization, warranting multi-batch replication for validation.

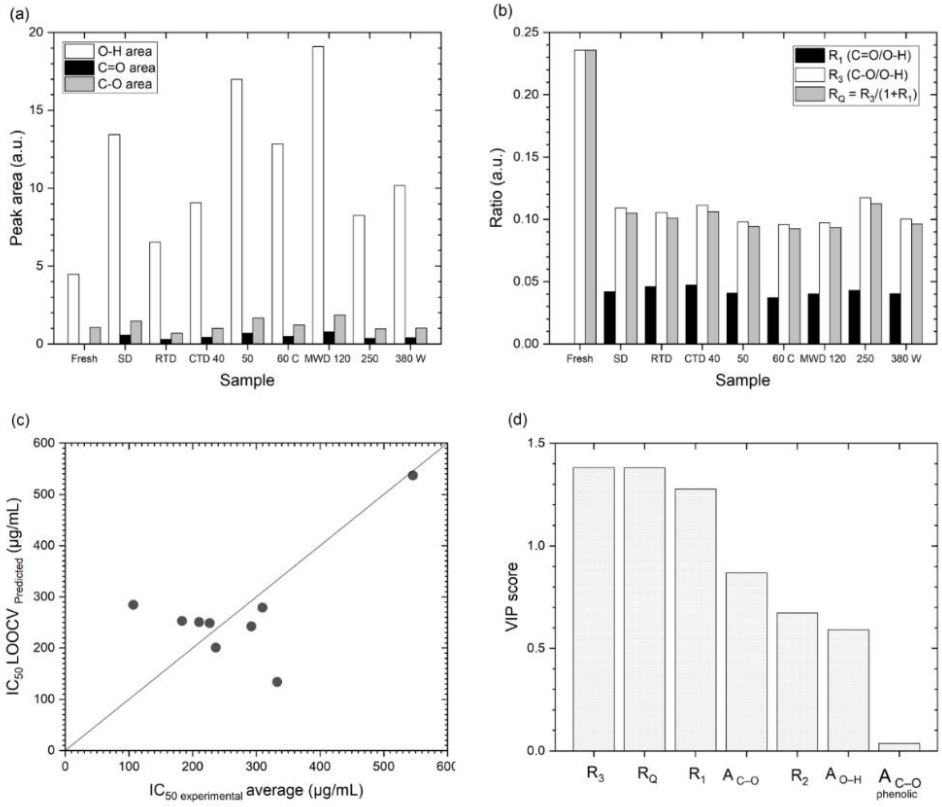

Figure 8 Quantitative FTIR analysis: (a) peak areas of O–H, C=O, and C–O; (b) ratio of R_1 to R_Q; (c) regression of PLS FTIR vs. antioxidant activity; and (d) FTIR ratio vs. VIP score.

Color attributes (L, a*, b*, ΔE, C and h°)

Fresh leaves exhibited low brightness and strong greenness (**Table 7** for details; L = 24.05 ± 0.04; a* = −6.72 ± 0.04; b* = 7.01 ± 0.03). Drying resulted in significant alterations across coordinates: L increased (highest at CTD 60 °C and MWD 250 W), a* shifted towards 0 (smallest loss at CTD 40 °C), and b* increased (maximum at CTD 60 °C). ΔE was smallest for CTD 40 °C (≈ 2.71; below the ~3 perceptual threshold) and highest for RTD; MWD was generally high.

Table 7 Changes in the color attributes of soursop leaves using various drying methods.

Sample	L	a*	b*	ΔE	C (Chroma)	h° (hue angle)
Fresh	24.05 ± 0.04^{d}	-6.72 ± 0.04^{h}	7.01 ± 0.03^{d}	-	9.71 ± 0.05^{a}	-46.22 ± 0.06^{a}
SD	25.84 ± 0.02^{c}	-1.58 ± 0.03^{c}	4.93 ± 0.02^{g}	5.83 ± 0.07^{f}	5.17 ± 0.04^{g}	-72.22 ± 0.18^{e}
RTD	15.61 ± 0.02^{f}	-1.72 ± 0.04^{d}	5.34 ± 0.02^{e}	9.95 ± 0.04^{a}	5.61 ± 0.03^{f}	-72.13 ± 0.28^{e}
CTD 40 °C	24.08 ± 0.59^{d}	-4.19 ± 0.02^{g}	7.86 ± 0.05^{b}	2.71 ± 0.04^{g}	8.91 ± 0.05^{c}	-61.91 ± 0.09^{b}
CTD 50 °C	19.35 ± 0.01^{e}	-2.53 ± 0.06^{f}	4.94 ± 0.05^{g}	6.63 ± 0.05^{e}	5.56 ± 0.07^{f}	-62.87 ± 0.27^{c}
CTD 60 °C	32.37 ± 0.03^{a}	-1.96 ± 0.02^{e}	8.87 ± 0.02^{a}	9.76 ± 0.03^{b}	9.08 ± 0.02^{b}	-77.52 ± 0.14^{f}
MWD 120 W	29.82 ± 0.03^{b}	-0.24 ± 0.03^{a}	5.05 ± 0.04^{f}	8.89 ± 0.02^{c}	5.06 ± 0.04^{g}	-87.24 ± 0.34^{h}
MWD 250 W	32.94 ± 0.05^{a}	-2.62 ± 0.04^{f}	7.50 ± 0.02^{c}	9.79 ± 0.09^{b}	7.94 ± 0.03^{d}	-70.71 ± 0.23^{d}
MWD 380 W	30.39 ± 0.03^{b}	-1.12 ± 0.06^{b}	6.95 ± 0.04^{d}	8.45 ± 0.02^{d}	7.04 ± 0.03^{e}	-80.82 ± 0.53^{g}

Note: Fresh samples were excluded from ANOVA ΔE due to 0 variance. Values are expressed as mean ± SD with n = 3; $p < 0,05$, Tukey's test.

The ΔE-IC_{50} plot demonstrated a weak-to-moderate correlation (R^2 = 0.265; **Figure 9**), indicating that visual color changes alone cannot fully explain antioxidant variation [83-85]. In contrast, the a* parameter exhibited a robust correlation with the FTIR R_Q ratio (R^2 = 0.733), where the loss of greenness (a* approaching 0) corresponded to a decrease in C–O/O–H (R_Q) and an increase in C=O (~1,734 cm^{-1}), reflecting phenolic depletion and carbonyl accumulation. These findings are consistent with those reported for *Strobilanthes crispus* and *Allium ursinum* [5,7,86-88]. In practice, CTD 40 °C was found to be capable of maintaining visual appearance (ΔE ≈ 2.7) but did not optimize phenolic preservation. Conversely, CTD 60 °C and MWD 380 W produced higher ΔE values (a noticeable sensory shift [84,89,90]) yet achieved superior phenolic retention and IC_{50} performance. However, it should be noted that color is determined by illumination conditions and instrument calibration, and it is unable to differentiate chlorophyll from phenolic degradation pathways. Therefore, cross-device color-space standardization is recommended.

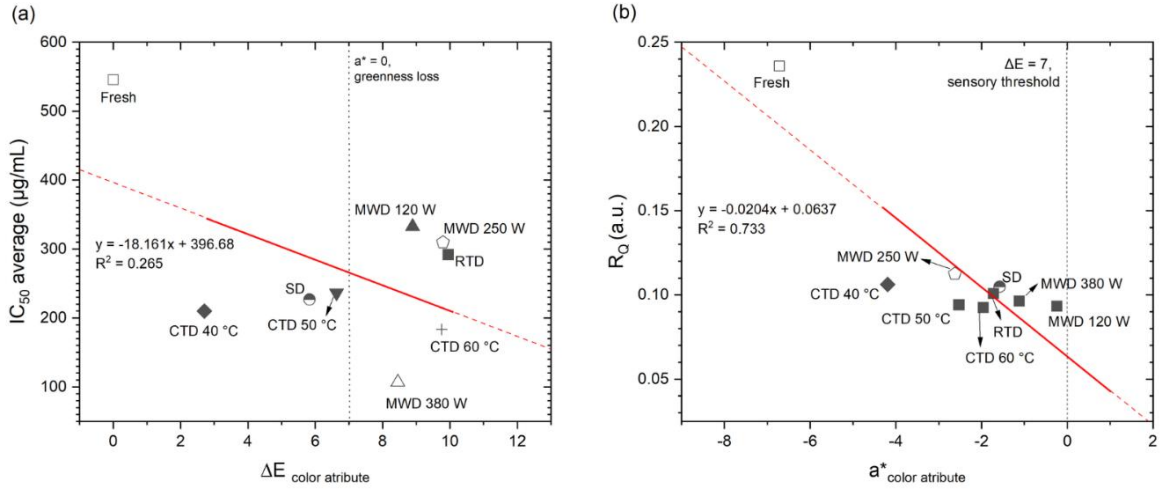

Figure 9 Correlation of color and function in soursop leaf.

Synthesis and practical implications

Overall, MWD 380 W represents an optimal process-product compromise: ≈ 4 min drying, low IC_{50}, and FTIR signatures consistent with phenolic retention; CTD 60 °C is a viable convective compromise. D_{eff} emerges as a kinetic surrogate, whereas bioactive quality should be predicted via FTIR ratios (R_Q/R_3) and, when required, a* as a rapid indicator. The integration of FTIR analysis with PLSR and VIP framework demonstrated potential for in-line quality control in tropical herbal processing.

Conclusions

This present study systematically integrated drying kinetics, spectroscopic indicators, and antioxidant response to establish a predictive framework for optimizing *Annona muricata* leaf drying. The findings can be summarized as follows: The first point to consider is that of kinetics and quality (scientific). The drying methods employed had a significant impact on both the kinetics and the quality of the product; the Midilli model yielded the optimal thin-layer fit (R^2 > 0.95; RMSE < 0.05), while the Jenna-Das model demonstrated efficacy under specific convective conditions. The effective moisture diffusivity (D_{eff}) exhibited an increase in accordance with both temperature and power, reaching a maximum at MWD 380 W, which resulted in an acceleration of up to ~225× in comparison to CTD 50 °C. A trade-off was observed, where CTD 40 °C maintained appearance (ΔE ≈ 2.7) but reduced phenolic retention, whereas CTD 60 °C and MWD 380 W yielded higher ΔE (> 8) yet superior FTIR ratios (R_Q, R_1 - R_3) and IC_{50} values; mid-power MWD (120 - 250 W) was detrimental. (ii) Structure-function relationships (scientific): The ΔE-IC_{50} correlation was weak to moderate, but a* exhibited a strong correlation with R_Q (R^2 ≈ 0.73). Furthermore, PLSR between FTIR indices and IC_{50} yielded $R^2_{\{LOOCV\}}$ ≈ 0.33 with VIP

emphasizing R_3 and R_Q. This validates FTIR ratios as non-destructive predictors of antioxidant preservation. In the third instance, the practical implementation of predictive quality control was demonstrated. The combination of the parameters ΔE and a* in conjunction with R_Q, functioned as expeditious indicators for real-time guidance. The integration of FTIR analysis with Partial Least Squares Regression (PLSR) and Variable Importance in Projection (VIP) transformed FTIR from a descriptive technique into an actionable inline or at-line quality control tool, thereby minimizing reliance on laborious assays and supporting green processing. The provision of actionable guidance on the practical implementation of drying processes is of paramount importance. MWD 380 W represented the optimal process-product compromise (≈ 4 min, low IC_{50}, favorable FTIR ratios), while CTD 60 °C was a reliable convective alternative, SD was rapid but inconsistent, and mid-power MWD should be avoided. In practice, D_{eff} can function as a kinetic gate, with R_Q and a* providing rapid bioactivity verification. It is recommended that future research endeavours extend the validation process to pilot and industrial scales. Additionally, there is a need to explore hybrid drying configurations, and integrate advanced chemometrics for real-time control.

Acknowledgements

The authors acknowledged the financial support from Universitas Diponegoro, Indonesia, 2025.

Declaration of Generative AI in Scientific Writing

The authors declare we have not used Artificial Intelligence (AI) tools in the creation of this.

CRediT Author Statement

Dessy Agustina Sari: Methodology, Investigation, Data curation, Writing - original draft, Visualization, Writing - review & editing; **Moh Djaeni:** Conceptualization, Supervision, Validation, Writing-review & editing; **Devi Yuni Susanti:** Formal analysis; **Joko Nugroho Wahyu Karyadi:** Visualization; **Olly Sanny Hutabarat:** Software; **Setia Budi Sasongko:** Software, Visualization; **Aji Prasetyaningrum:** Formal analysis; **Ching Lik Hii:** Methodology, Writing - review & Editing.

References

[1] B Bhattacharjee, K Sandhanam, S Ghose, D Barman and RK Sahu. *Market overview of herbal medicines for lifestyle diseases*. *In*: AK Dhara and SC Mandal (Eds.). Role of herbal medicines: Management of lifestyle diseases. Springer Nature, Singapore, 2024, p. 597-614.

[2] H Kaur, S Singh, SG Kanagala, V Gupta, MA Patel and R Jain. Herbal medicine - A friend or a foe of cardiovascular disease. *Cardiovascular and Hematological Agents in Medicinal Chemistry* 2024; **22(2)**, 101-105.

[3] D Buziak, SM Garland, DS Nichols, I Hunt and DC Close. *Astragalus membranaceus*: Impact of postharvest drying processes on yield and components of bioactive compounds. *Industrial Crops and Products* 2024; **209**, 117918.

[4] DH Ryu, JY Cho, M Hamayun, SH Lee, HH Cha, JH Jung and HY Kim. Optimizing drying time for *Centella asiatica* (L.) Urban: Metabolomic insights into dehydration effects on primary and secondary metabolites. *Chemical and Biological Technologies in Agriculture* 2025; **12(1)**, 26.

[5] J Lukinac and M Jukić. Influence of drying temperature on the organoleptic properties, antioxidant activity and polyphenol content in dried leaves of *Allium ursinum* L. subsp. *ucrainicum*. *Ukrainian Food Journal* 2022; **11(1)**, 2-26.

[6] HKF Oh, LF Siow and YY Lim. Approach to preserve phenolics in *Thunbergia laurifolia* leaves by different drying treatments. *Journal of Food Biochemistry* 2019; **43(7)**, e12856.

[7] INS Norasmadi, NN Zulkipli, S Lob, WZW Abdullah, MF Jusoh and A Mubarak. Effect of different drying methods on colour, total phenolic content, flavonoid content, and antioxidant activity retention of *Strobilanthes crispus* leaves. *Pertanika Journal of Tropical Agricultural Science* 2024; **47(4)**, 1157-1174.

[8] SB Rad, H Mumivand, S Mollaei and A Khadivi. Effect of drying methods on phenolic compounds and antioxidant activity of *Capparis spinosa* L. fruits. *BMC Plant Biology* 2025; **25(1)**, 133.

[9] K Mouhoubi, L Boulekbache-Makhlouf, K Madani, A Palatzidi, J Perez-Jimenez, I Mateos-Aparicio and A Garcia-Alonso. Phenolic

compounds and antioxidant activity are differentially affected by drying processes in celery, coriander and parsley leaves. *International Journal of Food Science & Technology* 2022; **57(6)**, 3467-3476.

[10] A Stupar, Ž Kevrešan, A Bajić, J Tomić, T Radusin, V Travičić and J Mastilović. Enhanced preservation of bioactives in wild garlic (*Allium ursinum* L.) through advanced primary processing. *Horticulturae* 2024; **10(4)**, 316.

[11] S Salehinia, F Didaran, S Aliniaeifard, S Zohrabi, S MacPherson and M Lefsrud. Green light enhances the phytochemical preservation of lettuce during postharvest cold storage. *PLoS One* 2024; **19(11)**, e0311100.

[12] M Kaveh, F Sharifian, A Alirezalu, S Keramat, B Gheisary, N Farhadi, MD Bachejak, E Rahmati and NN Balestani. Effect of ethanol and ultrasonic pretreatments on drying kinetics, quality, and physicochemical attributes of dried *Salvia officinalis*. *Biomass Conversion and Biorefinery* 2025; **15**, 30907-30923.

[13] GA Hernandez-Fuentes, OG Delgado-Enciso, EG Larios-Cedeño, JM Sánchez-Galindo, SG Ceballos-Magaña, K Pineda-Urbina, MA Alcalá-Pérez, NE Magaña-Vergara, J Delgado-Enciso, U Díaz-Llerenas, J Diaz-Martinez, I Garza-Veloz, ML Martinez-Fierro, IP Rodriguez-Sanchez and I Delgado-Enciso. Comparative analysis of infusions and ethanolic extracts of *Annona muricata* leaves from Colima, Mexico: Phytochemical profile and antioxidant activity. *Life* 2024; **14(12)**, 1702.

[14] S Oufquir, F Agouram, H Kabdy, MA Laaradia, K Oubella, B Abdelmoniim, A Rachida, S Garzoli and A Chait. Novel insights into the bioactive profile and therapeutic potentials of Indonesian *Annona muricata* leaves. *Chemistry & Biodiversity* 2025; **22(12)**, e01606.

[15] N Ismail, H Rajaratinam, KC Ghazali, SFM Salleh, WSFAW Ibrahim, MM Yahya and WZW Zain. The phytochemical components of Kelantan grown *Annona muricata* leaves and its anti-proliferative properties on MCF-7 breast cancer cells. *Sains Malaysiana* 2023; **52(10)**, 2785-2801.

[16] AG Peña, MR Alvarez, K Delica, PG Moreno, R Abogado, SJ Grijaldo, EL Salac, FM Deniega, M Basingan, CM Ravidas, F Heralde, GC Completo, I Padolina and R Nacario. Antioxidant and anticancer activities of *Annona muricata* L. and *Antidesma bunius* L. leaves, and molecular networking analysis using LC-MS/MS metabolomics. *South African Journal of Botany* 2022; **151**, 559-566.

[17] FHD de Andrade, RS de Araújo Batista, TBL Melo, FHA Fernandes, RO Macedo, FS de Souza and AG Wanderley. Characterization and compatibility of dry extract from *Annona muricata* L. and pharmaceutical excipients. *Journal of Thermal Analysis and Calorimetry* 2021; **143(1)**, 237-246.

[18] JS Mahesh, K Ramalakshmi and R Balakrishnaraja. Investigation of mass transfer parameters, phytochemical analysis of dried ripen graviola fruit (*Annona muricata*) and its comparative approach by using statistical tools: ANN and mathematical modelling. *Chemical Papers* 2023; **77(11)**, 7085-7098.

[19] J Shafana, S Kandasamy, M Shaji and K Kavivarshini. A study on the effect of microwave drying of herbs for determination of antioxidant activity. *AIP Conference Proceedings* 2021; **2387**, 020004.

[20] R ElGamal, OA Hamed, AM Rayan, C Liu, S Kishk, S Al-Rejaie and G ElMasry. Effect of convective and vacuum drying on some physicochemical and phytochemical characteristics of peppermint leaves. *AIMS Agriculture and Food* 2025; **10(1)**, 17-39.

[21] S Caliskan, H Oldenhof, R Brogna, B Rashidfarokhi, H Sieme and WF Wolkers. Spectroscopic assessment of oxidative damage in biomolecules and tissues. *Spectrochimica Acta Part A: Molecular and Biomolecular Spectroscopy* 2021; **246**, 119003.

[22] A Światły-Błaszkiewicz, J Gębalski, T Kaczmarek, D Załuski and B Kupcewicz. Exploring ED-XRF and ATR-FTIR spectroscopic techniques in medicinal plant research: A pilot study with *Scutellaria baicalensis* roots. *Journal of Pharmaceutical and Biomedical Analysis* 2025; **265**, 117008.

[23] F Martinez-Morales, AJ Alonso-Castro, JR Zapata-Morales, C Carranza-Álvarez and OH

Aragon-Martinez. Use of standardized units for a correct interpretation of IC_{50} values obtained from the inhibition of the DPPH radical by natural antioxidants. *Chemical Papers* 2020; **74(10)**, 3325-3334.

[24] W Hou, Z Duan and Y Yi. Effect of microwave drying on the phenolic content and color changes in different regions of persimmon slices. *Modern Food Science and Technology* 2024; **40(10)**, 259-269.

[25] JY Yap, CL Hii, SP Ong, KH Lim, F Abas and KY Pin. Degradation kinetics of carpaine and antioxidant properties of dried *Carica papaya* leaves as affected by drying methods. *International Journal of Food Engineering* 2022; **18(8-9)**, 593-602.

[26] S Kayacan-Cakmakoglu, I Atik, P Akman, I Doymaz, O Sagdıc and S Karasu. Effect of the different infrared levels on some properties of sage leaves. *Chemical Industry and Chemical Engineering Quarterly* 2023; **29(3)**, 235-242.

[27] M Pasławska, K Sala, A Nawirska-Olszańska, B Stępień and E Pląskowska. Effect of different drying techniques on dehydration kinetics, physical properties, and chemical composition of lemon thyme. *Natural Product Communications* 2020; **15(2)**, 1934578X2090452.

[28] J Deng, Z Chen, H Jiang and Q Chen. High-precision detection of dibutyl hydroxytoluene in edible oil via convolutional autoencoder compressed Fourier-transform near-infrared spectroscopy. *Food Control* 2025; **167**, 110808.

[29] AP Kusumadewi, R Martien, S Pramono, AA Setyawan, A Windarsih and A Rohman. Application of FTIR spectroscopy and chemometrics for correlation of antioxidant activities, phenolics and flavonoid contents of Indonesian *Curcuma xanthorrhiza*. *International Journal of Food Properties* 2022; **25(1)**, 2364-2372.

[30] NAZ Jinin, MAZ Benjamin and MA Awang. Drying kinetics and quality assessment of noodles from *Piper sarmentosum* Roxb. (Kaduk) leaves. *Malaysian Journal of Fundamental and Applied Sciences* 2024; **20(4)**, 835-851.

[31] KÇ Selvi. Investigating the influence of infrared drying method on Linden (*Tilia platyphyllos* Scop.) leaves: Kinetics, color, projected area, modeling, total phenolic, and flavonoid content. *Plants* 2020; **9(7)**, 916.

[32] S Verma, AB Usenov, DU Sobirova, SA Sultonova and JE Safarov. Mathematical description of the drying process of mulberry leaves. *IOP Conference Series: Earth and Environmental Science* 2022; **1112(1)**, 012012.

[33] RK Rout, A Kumar and PS Rao. A comparative assessment of drying kinetics, energy consumption, mathematical modeling, and multivariate analysis of Indian borage (*Plectranthus amboinicus*) leaves. *Journal of Food Process Engineering* 2024; **47(5)**, e14630.

[34] S Tan, Y Wang, W Fu, Y Luo, S Cheng and W Li. Drying kinetics and physicochemical properties of kumquat under hot air and air-impingement jet dryings. *Food Science and Biotechnology* 2022; **31(6)**, 711-719.

[35] Q Liu, X Jiang, F Wang, S Fan, B Zhu, L Yan, Y Chen, Y Wei and W Chen. Evaluation and process monitoring of jujube hot air drying using hyperspectral imaging technology and deep learning for quality parameters. *Food Chemistry* 2025; **467**, 141999.

[36] H Zhang, WZ Wang, XY Hu, J Wang, YY Han, XM Wang, XM Zhang, XY Guo, XY Huan, J Zhao, N Li, YF Wang and ZS Wu. Research on dynamic on-line monitoring method of moisture attribute in 3 honey-processed Chinese herbal slice based on in-situ general model. *Yaoxue Xuebao* 2023; **58(10)**, 2890-2899.

[37] T Belwal, C Cravotto, MA Prieto, PR Venskutonis, M Daglia, HP Devkota, A Baldi, SM Ezzat, L Gómez-Gómez, MM Salama, L Campone, L Rastrelli, J Echave, SM Jafari and G Cravotto. Effects of different drying techniques on the quality and bioactive compounds of plant-based products: A critical review on current trends. *Drying Technology* 2022; **40(8)**, 1539-1561.

[38] AS Eapen, YK Bhosale and S Roy. A review on novel techniques used for drying medicinal plants and its applications. *International Journal of Biomaterials* 2025; **2025(1)**, 4533070.

[39] B Kumar, SD Patle and SK Dewangan. Solar drying of ginger (*Zingiber officinale*) and turmeric

(*Curcuma longa*): A comprehensive review. *Solar Energy* 2025; **299**, 113748.

[40] S Chokngamvong and C Suvanjumrat. Study of drying kinetics and activation energy for drying a pineapple piece in the crossflow dehydrator. *Case Studies in Thermal Engineering* 2023; **49**, 103351.

[41] CL Recio-Colmenares, RB Recio-Colmenares, RF Conchas-Cedano, I Pilatowsky-Figueroa and CAG García. Data-driven hybrid CNN-LSTM neural networks for predicting drying kinetics of green tomatoes (*Physalis ixocarpa*) integrating mathematical models. *IEEE Access* 2025; **13**, 57413-57425.

[42] MI Maamar, M Badraoui, M Mazouzi and L Mouakkir. Mathematical modeling on vacuum drying of olive pomace. *Trends in Sciences* 2022; **20(2)**, 3822.

[43] FD Utari, DA Sari, L Kurniasari, AC Kumoro, M Djaeni and CL Hii. The enhancement of sappanwood extract drying with foaming agent under different temperature. *AIMS Agriculture and Food* 2023; **8(1)**, 214-235.

[44] O Dajbych, A Kabutey, Č Mizera and D Herák. Investigation of the effects of infrared and hot air oven drying methods on drying behaviour and colour parameters of red delicious apple slices. *Processes* 2023; **11(10)**, 3027.

[45] CA Osagiede and TM Stephen. Kinetic modelling of the drying behaviour of palm kernel (Dura species). *Journal of Science and Technology Research* 2024; **6(2)**, 237-249.

[46] S Baliyan, R Mukherjee, A Priyadarshini, A Vibhuti, A Gupta, RP Pandey and CM Chang. Determination of antioxidants by DPPH radical scavenging activity and quantitative phytochemical analysis of *Ficus religiosa*. *Molecules* 2022; **27(4)**, 1326.

[47] İ Gulcin and SH Alwasel. DPPH radical scavenging assay. *Processes* 2023; **11(8)**, 2248.

[48] TK Tepe. Convective drying of golden delicious apple enhancement: Drying characteristics, artificial neural network modeling, chemical and ATR-FTIR analysis of quality parameters. *Biomass Conversion and Biorefinery* 2024; **14(12)**, 13513-13531.

[49] K Altay, SN Dirim and AA Hayaloglu. Effects of different drying processes on the quality changes in Arapgir purple basil (*Ocimum basilicum* L.) leaves and drying-induced changes in bioactive and volatile compounds and essential oils. *Journal of Food Science* 2024; **89(12)**, 9088-9107.

[50] G Kumar, J Joshi, PS Rao and P Manchikanti. Effect of thin layer drying conditions on the retention of bioactive components in Malabar spinach (*Basella alba*) leaves. *Food Chemistry Advances* 2023; **3**, 100419.

[51] J Magnanensi, M Maumy-Bertrand, N Meyer and F Bertrand. New developments in sparse PLS regression. *Frontiers in Applied Mathematics and Statistics* 2021; **7**, 693126.

[52] T Mehmood, S Sæbø and KH Liland. Comparison of variable selection methods in partial least squares regression. *Journal of Chemometrics* 2020; **34(6)**, e3226.

[53] NN Mbegbu, CO Nwajinka and DO Amaefule. Thin layer drying models and characteristics of scent leaves (*Ocimum gratissimum*) and lemon basil leaves (*Ocimum africanum*). *Heliyon* 2021; **7(1)**, e05945.

[54] EE Wisdom, T Karikarisei and AH Cyrus. The dehydration kinetics of curry leaves (*Murraya koenigii rataceae*). *Indian Journal of Engineering* 2023; **20(53)**, e1ije1001.

[55] CM de Alcântara, IDS Moreira, MT Cavalcanti, RP Lima, HV Moura, RDS Neves, CAL Cassimiro, JJA Martins, FRDC Batista and EM Pereira. Mathematical modeling of drying kinetics and technological and chemical properties of *Pereskia sp.* leaf powders. *Processes* 2024; **12(10)**, 2077.

[56] OM Ferreira, VS Mendoza, THB Ferreira, RA Jordan and EJS Argandoña. Drying of *Xanthosoma sagittifolium* Schott leaves by heat pump and conventional dryer: And evaluation of bioactive compounds. *Journal of the Science of Food and Agriculture* 2025; **105(8)**, 4379-4387.

[57] F Ergün. Effects of drying methods on amounts of phenolic and flavonoid compounds and antioxidant capacity of *Plantago lanceolata* L. *The Journal of Animal and Plant Sciences* 2023; **33(1)**, 159-165.

[58] S Wahdaningsih, S Rizkifani, EK Untari and W Rinaldi. Effect of drying method on levels of antioxidant activity, total flavonoid levels, and

total phenol levels in ethanol extract of Bawang Dayak (*Eleutherine americana*) leaves. *Majalah Obat Tradisional* 2023; **28(1)**, 37-39.

[59] O Bualuang, DI Onwude and S Prangsri-Aroon. The effect of various drying strategies on the greenness, chlorophyll, bioactive compounds, antioxidant activity, and anti-tyrosinase of dried *Acanthus ilicifolius* L. leaves. *International Food Research Journal* 2022; **29(2)**, 416-432.

[60] K Mouhoubi, L Boulekbache-Makhlouf, W Mehaba, H Himed-Idir and K Madani. Convective and microwave drying of coriander leaves: Kinetics characteristics and modeling, phenolic contents, antioxidant activity, and principal component analysis. *Journal of Food Process Engineering* 2022; **45(1)**, e13932.

[61] A Hasizah, M Djalal, AA Mochtar and S Salengke. Fluidized bed drying characteristics of moringa leaves and the effects of drying on macronutrients. *Food Science and Technology* 2022; **42**, e103721.

[62] T Phull, P Phian and M Gupta. Kinetic simulation of convection drying for its effect on nutritional, functional, and phytochemical profiling of *Colocasia antiquorum* and *Nasturtium officinale* leaves of the Himalayan region. *Journal of Food Process Engineering* 2024; **47(2)**, e14548.

[63] A Kasara, OA Babar, A Tarafdar, T Senthilkumar, R Sirohi and VK Arora. Thin-layer drying of *sadabahar* (*Catharanthus roseus*) leaves using different drying techniques and fate of bioactive compounds. *Journal of Food Processing and Preservation* 2021; **45(2)**, e15140.

[64] A Ali, BL Chua, YH Chow and LH Tee. Quality and energy efficiency evaluation of *Rosmarinus officinalis* L. by intermittent and continuous microwave drying: Polyphenol composition, bioactive compounds quantification, antioxidant properties, physical characteristics, and energy consumption. *Journal of Food Process Engineering* 2023; **46(12)**, e14453.

[65] JG Yazar and E Demiray. Effects of conductive drying on drying kinetics and retention of bioactive compounds in mistletoe leaves. *Chemical Engineering and Processing - Process Intensification* 2023; **192**, 109490.

[66] S Hazra, N Nahar, SK Saha and R Chakraborty. Analysis of the influence of different drying processes on the quality attributes of orange peel. *Biocatalysis and Agricultural Biotechnology* 2024; **62**, 103429.

[67] M Ozdemir and S Karagoz. Effects of microwave drying on physicochemical characteristics, microstructure, and antioxidant properties of propolis extract. *Journal of the Science of Food and Agriculture* 2024; **104(4)**, 2189-2197.

[68] AM Castro, LE Díaz, MX Quintanilla-Carvajal, EY Mayorga and FL Moreno. Convective drying of feijoa (*Acca sellowiana* Berg): A study on bioactivity, quality, and drying parameters. *LWT* 2023; **186**, 115209.

[69] A Ghorbani, G Eghlima, M Farzaneh and A Rezghiyan. Effect of drying methods on mucilage, anthocyanin content, and antioxidant activity of black hollyhock (*Alcea rosea* var. *nigra*). *BMC Plant Biology* 2025; **25(1)**, 478.

[70] D Stephen, KJ Antony, PM Munusamy and T Deivanayagame. Impact of drying methods on the quality of bioactive components in tree tomato (*Cyphomandra betacae*). *Trends in Sciences* 2022; **19(2)**, 2060.

[71] SJ Fan, XY Zhang, Y Cheng, YX Qiu, YY Hu, T Yu, WZ Qian, DJ Zhang and S Gao. Extraction optimization of phenolic compounds from *Triadica sebifera* leaves: Identification, characterization and antioxidant activity. *Molecules* 2024; **29(14)**, 3266.

[72] Y Noui, A Lekbir, H Moussa, M Haffas, A Bousselma, S Hameurlaine, H Tahraoui, J Zhang, F Boufahja, H Bendif, A Amrane and W Elfalleh. Effects of microwave drying on physicochemical characteristics, microstructure and antioxidant activities of date fruit powders. *Journal of Food Measurement and Characterization* 2025; **19(8)**, 5554-5571.

[73] AG Nomi, H Handayani, RH Khuluk, AH Karomah, L Wulansari, ND Yuliana, E Rohaeti and M Rafi. Antioxidant activity and metabolite changes in *Centella asiatica* with different drying methods using FTIR- and quantitative HPLC-based metabolomics. *International Food Research Journal* 2024; **31(1)**, 228-238.

[74] P Thakur, R Saini, P Suthar, A Dhiman and S Kumar. Comparative evaluation of tray and microwave drying of black carrot (*Daucus carota*

L.): Effects on physicochemical, phytochemical and techno-functional properties. *Journal of the Indian Chemical Society* 2024; **101(10)**, 101327.

[75] JB Johnson, KB Walsh, M Naiker and K Ameer. The use of infrared spectroscopy for the quantification of bioactive compounds in food: A review. *Molecules* 2023; **28(7)**, 3215.

[76] AADL Santos, GF Leal, MR Marques, LCC Reis, JRDJ Junqueira, LL Macedo and JLG Corrêa. Emerging drying technologies and their impact on bioactive compounds: A systematic and bibliometric review. *Applied Sciences* 2025; **15(12)**, 6653.

[77] DC Fatmarahmi, RA Susidarti, RT Swasono and A Rohman. A development method of FTIR spectroscopy coupled with chemometrics for detection of synthetic drug adulterants of herbal products in quaternary mixture. *Journal of Applied Pharmaceutical Science* 2022; **12(3)**, 191-201.

[78] ZM Hamza, SA Kadhim and HH Hussain. Study of spectra physical for some samples of medical herbal by FTIR-ATR spectroscopy. *Journal of Pharmaceutical Negative Results* 2022; **13(1)**, 49-55.

[79] M Rafi, DA Tohib, A Saputra, Z Aziz and AH Karomah. FTIR-fingerprinting spectra combined with chemometrics analysis for distinguishing *Strobilanthes phyllostachya* leaves extracts and correlation with their antioxidant activity. *HAYATI Journal of Biosciences* 2025; **32(6)**, 1584-1591.

[80] R Ruslin, Y Yamin, I Irnawati, A Windarsih and A Rohman. FTIR spectra-based fingerprinting and chemometrics for rapid investigation of antioxidant activities of medicinal plants. *Journal of Research in Pharmacy* 2025; **29(4)**, 1522-1531.

[81] AA Bunaciu, S Fleschin and HY Aboul-Enein. FTIR spectroscopy used for study the thermal degradation of lard. *Egyptian Pharmaceutical Journal* 2021; **20(2)**, 166-172.

[82] T Chumroenphat, A Dechakhamphu, S Saensouk and S Siriamornpun. Drying conditions affected chemical profiles and health promoting properties of *Castanopsis piriformis* Hickel & A.Camus. *Food Chemistry: X* 2025; **29**, 102874.

[83] TCB Rigolon, FARD Barros, ÉNR Vieira and PC Stringheta. Prediction of total phenolics, anthocyanins and antioxidant capacity of blackberry (*Rubus* sp.), blueberry (*Vaccinium* sp.) and jaboticaba (*Plinia cauliflora* (Mart.) Kausel) skin using colorimetric parameters. *Food Science and Technology* 2020; **40(S2)**, 620-625.

[84] W Li, Y Zhang, H Deng, H Yuan, X Fan, H Yang and S Tan. *In vitro* and *in vivo* bioaccessibility, antioxidant activity, and color of red radish anthocyanins as influenced by different drying methods. *Food Chemistry: X* 2023; **18**, 100633.

[85] ZHT Cakmak, SK Cakmakoglu, E Avcı, O Sagdic and S Karasu. Ultrasound-assisted vacuum drying as alternative drying method to increase drying rate and bioactive compounds retention of raspberry. *Journal of Food Processing and Preservation* 2021; **45(12)**, e16044.

[86] J Zhang, J Zhang, L Zhang, Y Xue and K Zhang. Mechanistic insights into vegetable color stability: Discoloration pathways and emerging protective strategies. *Foods* 2025; **14(13)**, 2222.

[87] Y Huang, X Wang, Y Lyu, Y Li, R He and H Chen. Metabolomics analysis reveals the non-enzymatic browning mechanism of green peppers (*Piper nigrum* L.) during the hot-air drying process. *Food Chemistry* 2025; **464**, 141654.

[88] W Luo, J Guo, J Zhou, M Yang, and Y Wang. Mechanistic elucidation and establishment of drying kinetic models of differential metabolite regulation in *Rheum palmatum* during natural sun drying: An integrated physiology, untargeted metabolomics, and enzymology study. *Biology* 2025; **14(8)**, 963.

[89] L Zhang, C Zhang, Z Wei, W Huang, Z Yan, Z Luo, T Beta and X Xu. Effects of four drying methods on the quality, antioxidant activity and anthocyanin components of blueberry pomace. *Food Production, Processing and Nutrition* 2023; **5(1)**, 35.

[90] S Baibuch, P Zema, E Bonifazi, G Cabrera, ADCM Portocarrero, C Campos and L Malec. Effect of the drying method and optimization of extraction on antioxidant activity and phenolic of rose petals. *Antioxidants* 2023; **12(3)**, 681.